J. Phys. Chem. A **2004,** *108,* 9567−9572

An Elementary Reaction Kinetic Model of the Gas-Phase Formation of Polychlorinated Dibenzofurans from Chlorinated Phenols

Lavrent Khachatryan,[†] Ruben Asatryan,[‡] and Barry Dellinger*,[†]

Department of Chemistry, Louisiana State University, Baton Rouge, Louisiana 70803, and Department of Pharmaceutical and Toxicological Chemistry, Yerevan State Medical University, Yerevan 375025, Armenia

Received: May 24, 2004; In Final Form: August 18, 2004

A 30-reaction core kinetic model has been developed that accounts for the major features in the homogeneous formation of polychlorinated dibenzofurans (PCDF) from the high-temperature oxidation of 2,4,6-trichlorophenol (TCP). The core, purely gas-phase scheme provides agreement within a factor of 1.5−2 between experimental and calculated yields of PCDD/Fs using the REACT kinetic program. It is demonstrated that the formation of PCDF is due to the conversion of TCP to 2,4-dichlorophenol (DCP), which subsequently forms a keto resonance structure of the 2,4-dichlorophenoxyl radical ($DCP^•$). The conversion of TCP to DCP provides an ortho hydrogen that is necessary for the formation of PCDF. Ab initio calculations were utilized to calculate the activation energies of the key reactions involved in the gas-phase formation of PCDF.

I. Introduction

Combustion and thermal processes are generally recognized as the major sources of polychlorinated dibenzo-*p*-dioxins and dibenzofurans (PCDD/F or simply dioxins) in the environment.[1−3] A previously developed simple mechanism of gas-phase formation of PCDD from chlorinated phenols suggested that the gas-phase formation pathway was too slow to account for the concentrations of PCDD observed in full-scale combustors.[4] As a result, most research on the formation of PCDD/F in combustion sources has focused on surface-mediated formation.

The existing dioxin formation models [4−6] have been recently reexamined. On the basis of new literature data and the importance of stability of the phenoxyl radical, a modified approach was suggested to explain the gas-phase formation rates of dioxins by purely gas-phase reactions of phenoxyl radicals.[7−9] It has now been demonstrated that the potential yields of dioxins from gas-phase, chlorinated phenol precursors were grossly underestimated by the dioxin research community. As a result, it seems plausible to argue that gas-phase pathways for the formation of dioxins and furans deserve renewed consideration.

The concentration and reaction rate of phenoxyl radicals are the key parameters in the gas-phase formation of dioxins from chlorinated phenols. Our previous model of the gas-phase formation of PCDD from 2,4,6-trichlorophenol (TCP) indicated that the yields of PCDD are very sensitive to the steady-state concentration of the phenoxyl radical or, more precisely, to the phenoxyl-to-phenol ratio.[7,8] Unfortunately, there are no existing experimental data in the literature on the rate or yield of formation of chlorinated phenoxyl radicals from chlorinated phenols. This is in spite of the fact that their role in the formation of dioxins through radical−molecule or radical−radical pathways is widely discussed in the literature.[4−6,10,11]

On the basis of the newly available information concerning the nature and reactivity of non-chlorinated and chlorinated phenoxyl radicals, we recently reported our revisions to the original Shaub and Tsang (ST) model.[7,8] We added radical−radical reactions for the formation of PCDD and removed the erroneously fast reaction of chlorinated phenoxyl radicals with oxygen from the scheme. This modified (expanded) Shaub and Tsang model was developed on the basis of the experimentally observed formation of PCDD from the oxidation of TCP in the presence of dry air[5] and the oxidation of 2,4,6-TCP in the presence of 4% O_2 and hexane.[12] Formation of PCDFs was also observed in the latter study; however, a full mechanistic or reaction kinetic model that accounted for its origin has not been previously reported.

In this manuscript, we report the development of a modified model for the purely gas-phase formation of polychlorinated dibenzofurans (PCDFs) that is based on the experimentally observed formation of PCDF from the oxidation of 2,4,6-TCP in the presence of hexane.[12] This model is analogous to our previously reported model of the gas-phase formation of PCDD.[7,8] This model was subjected to numerical solution using the REACT kinetic program.[13] On the basis of our previously published experimental results[12] for the oxidation reaction of 2,4,6-TCP in the presence of hexane and the results of our model, we believe that PCDFs are formed as a result of the reactions of 2,4-dichlorophenol (DCP) generated by the displacement of chlorine from TCP by hydrogen atoms.[7,8] The resulting 2,4-DCP contains ortho hydrogen atoms that lead to the formation of PCDFs that were not possible from the direct reaction of 2,4,6-TCP.

II. Results: Development of a Reaction Kinetic Model for PCDF Formation

Table 1 presents our proposed reaction kinetic model for the gas-phase formation of PCDDs and PCDFs (designated D and DF in the model, respectively). It combines the PCDD formation submodel (rxns 1−13) discussed elsewhere[7] and a new additional PCDF formation submodel (rxns 14−30). The rate parameters for the reactions in the PCDD submodel were the same as in our previous model,[7] with the exception of the

---

* Corresponding author. Phone: 225 578 6759. Fax: 225 578 3458. E-mail: barryd@lsu.edu.

[†] Louisiana State University.

[‡] Yerevan State Medical University.

10.1021/jp047762r CCC: $27.50

TABLE 1: Reaction Kinetic Core Model for Formation of PCDD/Fs from TCP

no.	reaction step	rate constant[a]	units
1	$TCP \rightarrow TCP^\bullet + H^\bullet$	$3.16 \times 10^{15} \exp(-81\,500/RT)^{b}$	s^{-1}
2	$TCP + O_2 \rightarrow TCP^\bullet + HO_2^\bullet$	$2{\cdot}0 \times 10^{12} \exp(-41\,400/RT)^{c}$	$cm^3\ mol^{-1}\ s^{-1}$
3	$TCP^\bullet + TCP \rightarrow PD + Cl^\bullet$	$1.0 \times 10^{12} \exp(-26\,000/RT)^{d,e}$	$cm^3\ mol^{-1}\ s^{-1}$
4	$TCP + {}^\bullet OH \rightarrow TCP^\bullet + H_2O$	$10^{12\ d}$	$cm^3\ mol^{-1}\ s^{-1}$
5	$PD \rightarrow D + HCl$	$1.0 \times 10^{14} \exp(-45\,000/RT)^{d}$	s^{-1}
6	$PD + {}^\bullet OH \rightarrow PD^\bullet + H_2O$	$10^{12\ d}$	$cm^3\ mol^{-1}\ s^{-1}$
7	$TCP^\bullet \rightarrow PR1$	$2.5 \times 10^{12} \exp(-45\,000/RT)^{f}$	s^{-1}
8	$TCP^\bullet + OH \rightarrow PR2$	$10^{12\ d}$	$cm^3\ mol^{-1}\ s^{-1}$
9	$TCP^\bullet + TCP^\bullet \leftrightarrow P-P$	$k_8 = 8.64 \times 10^{11} \exp(1254/RT)^{g}$	$cm^3\ mol^{-1}\ s^{-1}$
		$k_{-8} = 3.16 \times 10^{15} \exp(-51\,000/RT)^{f}$	s^{-1}
10	$P-P \rightarrow PD^\bullet + Cl^\bullet$	$1.0 \times 10^{15} \exp(-44\,500/RT)^{f}$	s^{-1}
11	$PD^\bullet \rightarrow D + Cl^\bullet$	$1.0 \times 10^{12} \exp(-36\,500/RT)^{f}$	s^{-1}
12	$D + {}^\bullet OH \rightarrow PR3$	$10^{12\ d,h}$	$cm^3\ mol^{-1}\ s^{-1}$
13	$D \rightarrow PR4$	$3.16 \times 10^{15} \exp(-80\,000/RT)^{d}$	s^{-1}
14	$TCP + {}^\bullet H \rightarrow DCP + Cl^\bullet$	$1.5 \times 10^{13} \exp(-7500/RT)^{i}$	$cm^3\ mol^{-1}\ s^{-1}$
15	$DCP \rightarrow DCP^\bullet + H^\bullet$	$3.16 \times 10^{15} \exp(-81\,500/RT)^{b,j}$	s^{-1}
16	$DCP + O_2 \rightarrow DCP^\bullet + HO_2^\bullet$	$2.0 \times 10^{12} \exp(-41\,400/RT)^{c}$	$cm^3\ mol^{-1}\ s^{-1}$
17	$DCP + {}^\bullet OH \rightarrow DCP^\bullet + H_2O$	$10^{12\ d}$	$cm^3\ mol^{-1}\ s^{-1}$
18	$DCP^\bullet \rightarrow A^\bullet_{keto}$	$1.0 \times 10^{13\ j}$	s^{-1}
19	$A^\bullet_{keto} + A^\bullet_{keto} \leftrightarrow A_{keto} - A_{keto}$	$k_{19} = 8.64 \times 10^{11} \exp(1254/RT)^{g}$	$cm^3\ mol^{-1}\ s^{-1}$
		$k_{-19} = 1.0 \times 10^{15} \exp(-45\,400/RT)^{j}$	s^{-1}
20	$A_{keto}-A_{keto} \rightarrow Pr1$	$1.0 \times 10^{13} \exp(-23\,000/RT)^{j,e}$	s^{-1}
21	$A_{keto}-A_{keto}$ (interring) $\rightarrow A_{keto}-A_{enol}$	$1.0 \times 10^{13} \exp(-38\,000/RT)^{j}$	s^{-1}
22	$A_{keto}-A_{enol} + {}^\bullet OH \rightarrow A_{keto}-A^\bullet_{enol} + H_2O$	$10^{12\ d}$	$cm^3\ mol^{-1}\ s^{-1}$
23	$A_{keto}-A^\bullet_{enol} \rightarrow DF + {}^\bullet OH$	$1.0 \times 10^{12} \exp(-39\,500/RT)^{j}$	s^{-1}
24	$DCP^\bullet \rightarrow Pr2$	$2.5 \times 10^{12} \exp(-45\,000/RT)^{f}$	s^{-1}
25	$DCP^\bullet + {}^\bullet OH \rightarrow Pr3$	$10^{12\ d}$	$cm^3\ mol^{-1}\ s^{-1}$
26	$DF + {}^\bullet OH \rightarrow Pr4$	$10^{12\ d}$	$cm^3\ mol^{-1}\ s^{-1}$
27	$DF \rightarrow Pr5$	$3.16 \times 10^{15} \exp(-80\,000/RT)^{d}$	s^{-1}
28	$A_{keto}-A_{enol} \rightarrow A_{keto}-A^\bullet_{enol} + H^\bullet$	$3.16 \times 10^{15} \exp(-81\,500/RT)^{b,j}$	s^{-1}
29	$A_{keto}-A_{enol} + O_2 \rightarrow A_{keto}-A^\bullet_{enol} + HO_2^\bullet$	$2.0 \times 10^{12} \exp(-41\,400/RT)^{c}$	$cm^3\ mol^{-1}\ s^{-1}$
30	$A_{keto}-A_{enol} \rightarrow DF + H_2O$	$1.0 \times 10^{15} \exp(-59\,500/RT)^{j}$	s^{-1}

[a] Rate Constants: $k = A \exp[-Ea(\text{cal/mol})/RT]$. Symbols: TCP and $TCP^\bullet$ = 2,4,6-trichlorophenol and 2,4,6-trichlorophenoxy radical, respectively. PD and $PD^\bullet$ = predioxin and radical, respectively, as assigned in ref 4, D-chlorinated dioxin. DCP and $DCP^\bullet$ = 4,6-dichlorophenol and 4,6-dichlorophenoxy radical, respectively. $A_{keto}^\bullet$ = resonance structure of DCP· (keto form). $A_{keto}-A_{keto}$ and $A_{keto}-A_{enol}$ = bisketo and keto−enol dimer forms of A·, respectively. DF = polychlorinated dibenzofuran (PCDF). Pr and PR are not specified products. [b] Reference 11, see also text. [c] References 7, 8; a fitted value for the preexponential factor, 6×10^{13} $cm^3\ mol^{-1}\ s^{-1}$, was used on the basis of the recommendation in ref 7. [d] Reference 4. [e] Reference 22. [f] References 7, 8. [g] Reference 19. [h] Reference 35. [i] Reference 18. [j] See text.

activation energy of rxn 1 (as well as for the similar rxns 15 and 28) which was reduced by ~5 kcal/mol to 81.5 kcal/mol. This reduction is based on the new suggestions reported in the literature,[11] as well as on our own ab initio calculations for *o*- and *p*-chlorophenols as well as phenol.

Ab initio calculations of the subject species were performed using *Gaussian 98*[14] at the B3LYP/6-31G(d,p) theoretical level

$$C_6H_5OH \leftrightarrow C_6H_5O^\bullet + H^\bullet$$
$$\Delta E = 81.35 \text{ kcal/mol } (\Delta H = 82.68 \text{ kcal/mol})$$

$$p\text{-}Cl-C_6H_4OH \leftrightarrow Cl-C_6H_4O^\bullet + H^\bullet$$
$$\Delta E = 80.73 \text{ kcal/mol } (\Delta H = 82.05 \text{ kcal/mol})$$

$$o\text{-}Cl-C_6H_4OH \leftrightarrow Cl-C_6H_4O^\bullet + H^\bullet$$
$$\Delta E = 80.10 \text{ kcal/mol } (\Delta H = 81.43\text{kcal/mol})$$

The value of ΔH is closely related to the activation energy for the hydroxyl−hydrogen dissociation reaction to form the phenoxyl radical.

We focus our attention to the reactions of the PCDF submodel, rxns 14−30. Some of the reaction rate parameters were assigned on the basis of the analogous reactions in the ST model (rxns 15, 17, 22, 25−27)[4−6] and our revised ST model (rxns 16, 24).[7] We will explicitly discuss the contribution of DCP as a precursor of PCDF formation, as well as the role of the 2,4-dichlorophenoxyl radical ($DCP^\bullet$) molecule and the corresponding radical−radical pathways leading to PCDF. The key steps in the more favorable radical−radical pathways to PCDF are the reaction sequence 19 and 21−23. The formation (from DCP) and consumption of $DCP^\bullet$ (rxns 15−17, 18, 25) follow reaction sequences analogous to those previously developed for 2,4,6-DCP•.[7,8] The reactions of $DCP^\bullet$ resulting in the formation of PCDF are discussed in more detail (vide infra).

II.1. Formation of 2,4-Dichlorophenol Molecule and Radical. It has been previously argued that chlorinated phenols, for which both ortho carbon atoms are chlorine-bearing sites, cannot form PCDFs via a radical−radical pathway.[5,15] This is because proposed pathways involve a tautomerization of an ortho phenyl hydrogen of the keto mesomer to a phenolic hydrogen in the enol form. When both ortho sites are chlorinated, a phenoxyl−chlorine bond would have to be formed in the enol form that is energetically unstable. Thus, it seems clear that only chlorinated phenols containing at least one ortho hydrogen can form PCDFs. This was previously demonstrated in the experimental studies of the oxidation of TCP in which only 1,3,6,8- and 1,3,7,9-TCDD were formed.[5]

However, addition of hexane to the TCP oxidation resulted in the formation of 1,3,6,8- and 2,4,6,8-TCDF.[12] We attribute this to the formation of 2,4-DCP by displacement of $Cl^\bullet$ (or abstraction) from TCP by hydrogen atoms, which are in increased supply with the addition of hexane to the system.

Our previous model of the formation of PCDD from TCP resolves some of the impacts of hexane addition and demonstrates why the addition of hexane increases the yield of PCDD.[8] The hexane oxidation submodel provides not only the generation

TABLE 2: Estimated Heats for the Reaction TCP + TCP$^•$ → PF + OH Using Non-Empirical HF/3-21G and AM1, PM3 Methods

TCP	+TCP$^•$	→PF^a	+$^•$OH	ΔH_{rxn} (kcal/mol)
−38.32 (AM1)	−13.74	+9.94	0.64	+62.64
−39.43 (PM3)	−17.23	−0.78	2.84	+58.72
−1674.317 042^b	−1673.731 04	−3272.976 10	−74.970 22	+63.85

[a] Prefuran, PF, by analogy of PD.[4] [b] Ab initio results, total energies in hartree units; 1 hartree = 627.5 kcal/mol.

of main chain carriers such as hydroxyl radicals but also hydrogen atoms. Hexane increases the probability of DCP formation by the reaction H$^•$ + TCP → DCP + Cl$^•$. The displacement of Cl$^•$ by H$^•$ (or abstraction of Cl by H followed by H addition) is also well-documented experimentally in the gas-phase pyrolyses of 2,6-DCP, where one of the major products was 2-chlorophenol,[16] and in the gas-phase pyrolysis of 2-chlorophenol performed recently in our laboratory,[17] where phenol was a major product. These facts suggest that the formation of DCPs with at least one ortho hydrogen is highly favorable during gas-phase pyrolysis of a mixture of TCP, O_2, and hexane in the middle- and high-temperature regimes where these reactions are energetically favorable.

By analogy to the reaction H$^•$ + Cl−C_6H_5 → C_6H_6 + Cl$^•$, which is exothermic by 15.8 kcal/mol and has a rate constant of 1.5×10^{13} exp(−7500/*RT* cal/mol) cm^3/mol•s,[18] we assign the same value for DCP formation from TCP (Table 1, rxn 14). The chlorine abstraction reaction by H$^•$ with an activation energy of <9 kcal/mol and further annihilation of the resulting radical by H$^•$ may also lead to the formation of DCP in our reaction system. This reaction sequence has not been included in our current model.

II.2. Radical−Molecule Pathway to PCDF. The formation of TCDF by a radical−molecule pathway analogous to that for the formation of PCDD requires a displacement of $^•$OH from the chlorinated phenol by the chlorinated phenoxyl radical.

Ab initio Hartree−Fock calculations presented in Table 2 in accordance with AM1 and PM3 results indicated that, because of the high endothermicity for PCDF formation through radical−molecule reaction (TCP + TCP·), this channel must be considered implausible.

II.3. Radical−Radical Pathway to PCDF. The electronic structure and properties of the phenoxyl radical and its chlorinated derivatives were studied not only experimentally[19−21] but also using a variety of semiempirical and nonempirical theoretical methods.[7,8,22,23] Under valence bond theory, the electronic structure of 2,4-DCP$^•$ can be presented as a superposition of three principal resonance structures: oxygen-centered as well as ortho- and para-carbon-centered phenoxyl radicals. The contribution of these different resonance structures to the actual structure of the radical can be estimated from a molecular orbital theory viewpoint on the basis of the localization of corresponding spin densities on radical active centers.[22,23]

The 2,4-DCP$^•$ can be represented as a superposition of two resonance structures (viz., the oxygen-centered resonance structure, DCP$^•$, and the carbon-centered resonance structure, A$^•$keto, as in rxn 18). The ortho-carbon-centered radical structure of the 2,4-DCP$^•$ is the direct precursor of PCDFs. As resonance structures, there are no formal reactions for their interconversion within the valence bond theory of chemical reactions. However, to emphasize the interconversion, we include this process in the model as rxn 18. Furthermore, there may be conditions when the reactions occur on surfaces, in which these moieties are separately identifiable chemical species rather than resonance structures. Inclusion of rxn 18 facilitates future discussions of surface-mediated PCDD and PCDF formation.

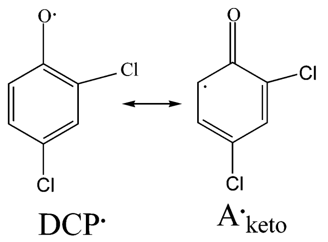

(18)

The rate constant of the self-condensation reaction (rxn 19) of two keto forms of phenoxyl radicals is assigned the same value as for nonchlorinated phenoxyl radicals, $k_{19} = 8.64 \times 10^{11}$ exp(1254/*RT*) cm^3 mol^{-1} s^{-1}.[19,21] It has been reported that mono- and trichlorination of phenoxyl radicals does not affect significantly the reactivity of phenoxyl radicals.[11,22]

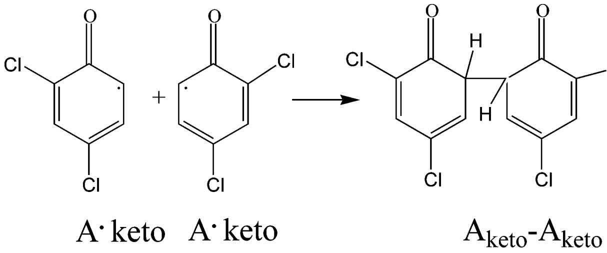

(19)

Recently, the dimerization of phenoxyl radicals has been studied in the context of biomedical consequences[24] and dibenzofuran formation mechanisms[25]. In these studies, the possible formation of intermediate *π*-complexes via phenoxyl radical coupling is considered within a thermodynamic framework.

We have previously demonstrated that, within a reaction kinetic framework using the B3LYP/6-31G(d) level of theory, conversion of an A_{keto}−A_{keto} dimer into an ether species (O/para C in rxn 20) can efficiently proceed.[22]

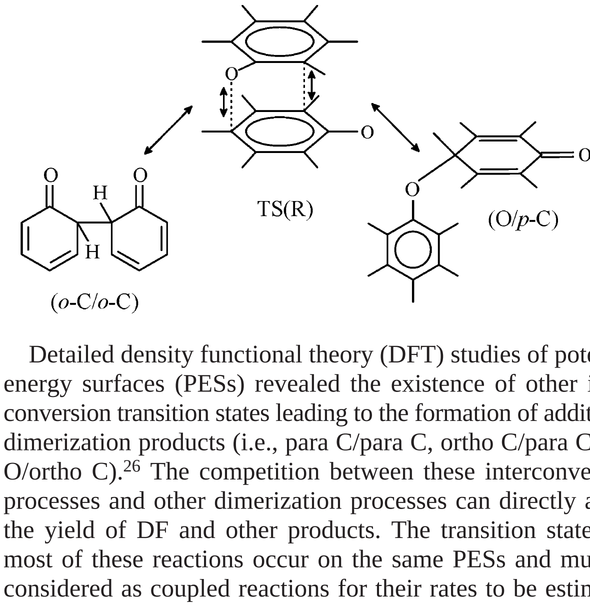

(20)

Detailed density functional theory (DFT) studies of potential energy surfaces (PESs) revealed the existence of other interconversion transition states leading to the formation of additional dimerization products (i.e., para C/para C, ortho C/para C, and O/ortho C).[26] The competition between these interconversion processes and other dimerization processes can directly affect the yield of DF and other products. The transition states for most of these reactions occur on the same PESs and must be considered as coupled reactions for their rates to be estimated properly.[26]

The rate constant for rxn 20 is assigned as $k_{20} = 1.0 \times 10^{13}$ exp(−23 000/*RT*) cal mol^{-1} s^{-1} where the activation energy is based on our DFT calculations[22] and a preexponential factor was calculated as $1.0 \times 10^{13.05}$ s^{-1} according to the formula $\Delta S^{\#} = 1.0 \times 10^{13.55}$ exp($\Delta S^{\#}/R$) from transition state theory

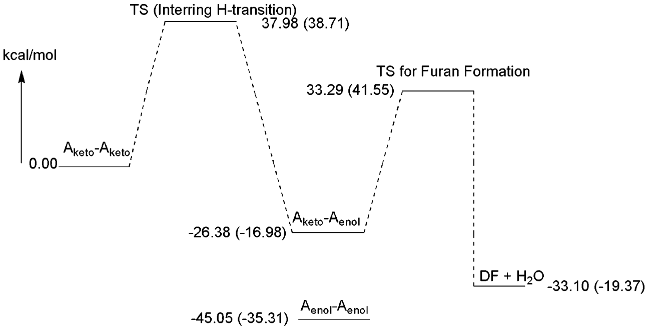

Figure 1. The results of ab initio and AM1 (in parentheses) calculations for total reaction: $A_{keto}-A_{keto} \Rightarrow DF + H_2O$.

(TST) for unimolecular reactions.[27] The value of $\Delta S^{\#}$ was = −2.29 cal/mol·K. However, the fate of the $A_{keto}-A_{keto}$ radical−radical adduct depends primarily on competition with the dissociation reaction, rxn −19, rxn 20, and the PCDF formation sequence, rxns 21−23.

The back dissociation reaction, rxn −19, of $A_{keto}-A_{keto}$ is significant.[7,8,28] The barrier to decomposition for rxn −19 was assigned as 43 000 cal/mol on the basis of the analogous reaction of nonchlorinated ortho C/ortho C adduct species extracted from ref 11 and assuming a preexponential factor of $\sim 10^{15}$ s^{-1}. When the assigned rate parameters are used, the ratio of the reaction rates of rxn 20 and rxn −19 is $\sim 6.7 \times 10^3$ at 750 C. The conversion rate of the $A_{keto}-A_{keto}$ adduct to the partially enolized form (rxn 21) is comparable to the back dissociation reaction.

II.4. Closed-Shell Pathways to PCDF (Rxn 21). We performed additional calculations concerning the reactions of the partially enolized $A_{keto}-A_{enol}$ structure (rxn 21) and the doubly enolized $A_{enol}-A_{enol}$ structure of the bisketo adduct ($A_{keto}-A_{keto}$, rxns 21′ and 23′, not shown in Table 1), as well as the PCDF formation reaction, rxn 23.

$$A_{keto}-A_{keto} \rightarrow A_{enol}-A_{enol} \qquad \text{(rxn 21′)}$$

$$(A_{enol}-A_{enol}) \rightarrow \text{DF (2,4,6,8)} + H_2O \qquad \text{(rxn 23′)}$$

For simplicity, we performed calculations on nonchlorinated species and assumed that the presence of additional chlorine atoms did not distort the aromatic ring.[22] Our Hartree−Fock (HF/3-21G) calculation results suggest that double enolization of the bisketo form (rxn 21′) and further conversion of the bisenol form to PCDF with the elimination of water (rxn 23′) are energetically unfavorable (cf. Figure 1). Thermodynamically, the conversions of bisketo to keto−enol or bisenol forms are exothermic and favorable; however, our ab initio results indicate that there are large activation barriers for the conversion to PCDF via the unimolecular elimination of H_2O. From the keto−enol structure, the barrier to PCDF formation according to HF/3-21G(d) is 59.50 kcal/mol. From the bisenol structure, the barrier will be ca. 78 kcal/mol using the same transition state for the keto−enol form, Figure 1 (In the latter case, we could not find a stable transition state).

The difficulties of the conversion of bisenol into DF have been previously discussed.[28] It is already documented[29] that the formation of DF via dehydroheterocyclization of 2,2′-dihydroxy-3,3′,5,5′-tetra-*tert*-butylbiphenyl in acetic acid media proceeds only when it is catalyzed by bromine.

Despite the failure of the Hartree−Fock results for estimation of benzene dimerization due to the neglect of electron correlation effects,[30] this method can be expected to be reliable in isomerizations (tautomerization) of closed-shell systems such as $A_{keto}-A_{keto}$. The HF approximation gives reliable results that are comparable to DFT calculations in the case of open-shell ipso addition reactions of chlorinated phenoxyl radicals with corresponding molecules.[22]

TABLE 3: Calculated by HF/3-21G Energies for Rxn 23, $A_{keto}-A_{enol}^{\bullet} \rightarrow DF + OH$

$A_{keto}-A_{enol}^{\bullet}$	TS	DF + OH
−2433.271 682[a]	−2433.208 501	−2433.213 851

[a] Total energies in hartree units; 1 hartree = 627.5 kcal/mol.

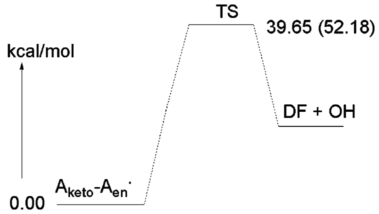

Figure 2. Calculated by HF/3-21G and AM1 (in parentheses) profile of rxn 23: $A_{keto}-A_{en}^{\bullet} \Rightarrow DF + OH$.

The HF/3-21G ab initio and AM1 calculations give activation energies of 37.98 and 38.71 kcal/mol, respectively, for the conversion of the bisketo to the keto−enol form through a transition state for the inter-ring H transfer. A preexponential factor for rxn 21 was calculated as $1.0 \times 10^{12.33}$ s^{-1} (fitted value in the model is $1.0 \times 10^{13.0}$ s^{-1}, Table 1) on the basis of the formula $\Delta S^{\#} = 1.0 \times 10^{13.55} \exp(\Delta S^{\#}/R)$ from TST for unimolecular reactions.[27] The value of $\Delta S^{\#}$ was−5.60 cal/mol·K.

In contrast, the barrier to the intra-ring H transfer process according to AM1 result is 66.80 kcal/mol. The analogous type of isomerization reaction of methylcyclohexadienone to *o*-cresol was assigned an activation energy of 32 kcal/mol in ref 31. Because both the inter-ring and intra-ring enolizations have high activation energies, we also consider the radical−molecule reaction sequences 22 and 23 (vide infra).

II.5. Open-Shell Pathway to PCDF (Reaction 23). Ab initio HF/3-21G simple basis calculations for rxn 23 are summarized in Table 3**.**

An activation energy of 39.65 kcal/mol is calculated for the inter-ring displacement rxn 23 (Figure 2). This activation energy is still relatively large and, in addition, requires abstraction of a hydrogen atom in rxn 22 for $A_{keto}-A_{enol}^{\bullet}$ to be formed.

Thus, the reaction sequence 22/23, as well as the unimolecular reaction with a barrier of 59.50 kcal/mol from the keto−enol structure (Figure 1, rxn 30 in Table 1), appear to be the preferred routes to PCDF formation.

III. Discussion: Comparison of Model and Experimental Results

The mechanism in Table 1 (rxns 1−30) was used to assess the gas-phase formation of PCDF through computer simulation via a simple ordinary differential equation system solver: REACT Kinetic Program.[13] The input conditions were the initial species concentrations: 2,4,6-TCP = 1.60×10^{-10} mol/cm^3 in the presence of 4% O_2 and 300 ppm hexane for a reaction time of 2.0 s, over a temperature range of 950 to1150 K.[12] The outputs were the final concentrations of all species in the mechanism.

For simplicity and the purpose of demonstration, we did not include the hexane oxidation submodel. A relatively complete model for the gas-phase formation of PCDD for exactly the same conditions is discussed elsewhere[8] using the CHEMKIN combustion package. Because initial hydrogen atoms are needed to convert TCP to DCP, we used a hydroxyl-radical-to-

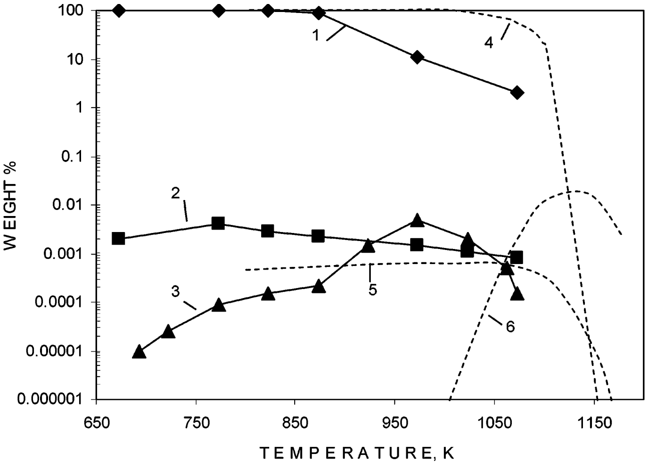

Figure 3. Comparison of results of the core model (30 rxns) solution (REACT) and experimental results for the oxidation of 2,4,6-TCP.[12] Curves 1, 2, and 3: experimental results for consumption of 2,4,6-TCP, accumulation of dioxins, and furans, respectively. Curves 4, 5, and 6: model results for 2,4,6-TCP decomposition, dioxin, and furan formation, respectively, via homogeneous, gas-phase reactions (rxns 1−30 excluding rxn 19 and with optimized A_2, A_{16}, $A_{29} = 6.0 \times 10^{13}$ cm^3•mol^{-1} s^{-1}.[7]).

hydrogen-atom ratio of [OH]/[H] ≈ 80 from our previous work[8] to mimic the influence of the hexane oxidation process as a generator of these species. It has been shown that the behavior of the temperature dependence of H atoms is similar to that of OH radicals over the temperature range considered (900−1100 K).[8] The concentration of hydroxyl radicals (mole/L) was calculated by $[OH] = 10^{-1.7} \times \exp(-35.0\ \mathrm{kcal/mol}/RT)$.[4]

Reasonable agreement between calculated and experimental data was achieved using the rate parameters in Table 1. The preexponential factor of the rate of the initiation of TCP by reaction with oxygen of 6.0×10^{13} cm^3/mol•s in rxns 2, 16, and 29 was the previously estimated reaction parameter from the recommended values from our PCDD formation model.[7] It is close to the value of 1.0×10^{14} cm^3/mol•s used in the model developed for the thermal oxidation of phenol.[32−34] This simple parametric adjustment is reasonable, because a similar acceleration can be reached by making small changes in the rates of the oxidation reactions of hexane, including modest wall effects, or considering the influence of impurities.

In Figure 3, the theoretical curves for both TCP decomposition and PCDF formation are shifted approximately 100 K higher in temperature than the experimental data. The maximum model yield of PCDF is 0.009 wt % at 1100 K, in reasonable agreement with the maximum experimental yield of 0.005 wt % at 975 K, despite the 100−125 K shift in temperature. The experimental data for both PCDD and PCDF show formation at very low temperatures from 650 to 900 K. We have previously attributed this low-temperature formation to wall effects or impurities in the reactants that initiate small amounts of TCP decomposition at these low temperatures. Consequently, our model can only be considered appropriate for the homogeneous reaction of pure TCP above 950 K.

The higher-temperature formation of PCDF in higher yields compared to PCDD is not surprising and has been previously mentioned in several publications reporting the pyrolysis of chlorophenols[12,17] at short reaction times (viz., 2.0 s). Including the reverse reaction (rxn −19) with $k_{-19} = 1.0 \times 10^{15} \exp(-43\,000/RT)$ cal mol^{-1} s^{-1} does not affect the yields of PCDF. Within the assigned rate coefficients for our model, $A_{keto}-A_{keto}$ easily undergoes interconversion by rxn 20 or, by radical chain reactions 22/23, converts to PCDF. Therefore, the precise reaction parameters of these reactions become an issue.

IV. Concluding Remarks

(1) A 30-step core reaction model has been developed to explain the purely gas-phase formation of PCDD/F from the gas-phase oxidation of 2,4,6-trichlorophenol (TCP). Ab initio calculations were utilized to calculate the activation energies of the key reactions involved in the gas-phase formation of PCDF.

(2) The formation of PCDF is contingent on formation of 2,4-dichlorophenol (DCP) by the displacement (abstraction) of an ortho chlorine from TCP by $H^•$ (rxn 14). Once an ortho hydrogen appears, the radical−radical pathway to PCDF formation is available. The initially formed keto structure, $A^•_{keto}$. then undergoes radical−radical recombination to form a bisketo adduct (rxn 19). Subsequent monoenolization of the adduct (rxn 21) followed by further radical chain reactions (rxns 22 and 23) results in the formation of PCDF.

(3) Reasonable agreement between calculated yields (REACT kinetic solver) and experimental yields of PCDF is achieved above 950 K using this PCDF formation pathway in combination with excluding the reactions of chlorinated phenoxyl radicals with oxygen, as was done in our previous model of PCDD formation.[7,8] The model does not satisfactorily explain PCDF formation at low temperatures. A question is raised concerning the contribution of surfaces or reactive impurities in the mechanism of PCDD/F formation at low temperatures.

(4) For the first time, a reaction kinetic mechanism for the formation of PCDF from chlorinated phenols has been developed with modest, but reasonable, agreement with experimental results. However, the uncertainty of numerous reaction rate parameters for chlorinated hydrocarbon species suggests that additional attention be paid to calculating and estimating these parameters.

Acknowledgment. This work was partially support by NSF grant 9996085 and the Patrick F. Taylor Chair Foundation. We gratefully acknowledge Drs. Sherrill and Mulholland (ref 25) for providing preliminary data on PCDD/F formation.

References and Notes

(1) Altwicker, E. R.; Schonberg, J. S.; Kondury, R. K. N. V.; Milligan, M. S. *Hazard. Waste Hazard. Mater.* **1990**, *7* (1), 73.

(2) Huang, H.; Buekens, A. *Chemosphere* **1995**, *31*, 4099.

(3) Fiedler, H. *Environ. Eng. Sci.* **1998**, *15* (1), 49.

(4) Shaub, W. M.; Tsang, W. *Environ. Sci. Technol.* **1983**, *17*, 721.

(5) Sidhu, S. S.; Maqsud, L.; Dellinger, B.; Mascolo, G. *Combust. Flame.* **1995**, *100* (1/2), 11.

(6) Huang, H.; Buekens, A. *Chemosphere* **1999**, *38*, 1595.

(7) Khachatryan, L.; Asatryan, R. S.; Dellinger, B. *Chemosphere* **2003**, *52*, 695.

(8) Khachatryan, L.; Burcat, A.; Dellinger, B. *Combust. Flame* **2003**, *132*, 406.

(9) Babushok, V.; Tsang, W. *Chemosphere* **2003**, *51*, 1023.

(10) Louw, R.; Grotheer, H. H.; Kanters, M. J.; Wiater, I. *Organohalogen Compd.* **1996**, *27*, 26.

(11) Louw, R.; Ahonkhai, S. I. *Chemosphere* **2002**, *46*, 1273.

(12) Sidhu, S. S.; Dellinger, B. *Organohalogen Compd.* **1997**, *31*, 469.

(13) Bozzelli, J. W. *J. Chem. Educ.* **2000** *77*, 165.

(14) Frisch, M. J.; Trucks, G. W.; Schlegel, H. B.; Scuseria, G. E.; Robb, M. A.; Cheeseman, J. R.; Zakrzewski, V. G.; Montgomery, J. A., Jr.; Stratmann, R. E.; Burant, J. C.; Dapprich, S.; Millam, J. M.; Daniels, A. D.; Kudin, K. N.; Strain, M. C.; Farkas, O.; Tomasi, J.; Barone, V.; Cossi, M.; Cammi, R.; Mennucci, B.; Pomelli, C.; Adamo, C.; Clifford, S.; Ochterski, J.; Petersson, G. A.; Ayala, P. Y.; Cui, Q.; Morokuma, K.; Malick, D. K.; Rabuck, A. D.; Raghavachari, K.; Foresman, J. B.; Cioslowski, J.; Ortiz, J. V.; Stefanov, B. B.; Liu, G.; Liashenko, A.; Piskorz, P.; Komaromi, I.; Gomperts, R.; Martin, R. L.; Fox, D. J.; Keith, T.; Al-Laham, M. A.; Peng, C. Y.; Nanayakkara, A.; Gonzalez, C.; Challacombe, M.; Gill, P. M.

W.; Johnson, B. G.; Chen, W.; Wong, M. W.; Andres, J. L.; Head-Gordon, M.; Replogle, E. S.; Pople, J. A. *Gaussian 98*, revision A.11; Gaussian, Inc.: Pittsburgh, PA, 2001.

(15) Wiater, I.; Louw, R. *Organohalogen Compd.* **1999**, *41*, 77.

(16) Akki, U.; Mulholland, J. A. *Organohalogen Compd.* **1997**, *31*, 475.

(17) Evans, C. E.; Dellinger, B. *Environ. Sci. Technol.* **2003**, *37*, 1325.

(18) Ritter, E. R.; Bozzelli, J. W. *J. Phys. Chem.* **1990**, *94*, 2504.

(19) Berho, F.; Lesclaux, R. *Chem. Phys. Lett.* **1997**, *279*, 289.

(20) Platz, J.; Nielsen, O. J.; Wallington, T. J.; Ball, J. C.; Hurley, M. D.; Straccia, A. M.; Schneider, W. F.; Sehested, J. J. *J. Phys. Chem. A* **1998**, *102*, 7964.

(21) Tao, Z.; Li, Z. K. *Int. J. Chem. Kinet.* **1999**, *31*, 65.

(22) Asatryan, R.; Davtyan, A.; Khachatryan, L.; Dellinger, B. *Organohalogen Compd.* **2002**, (Dioxin 2002), *56*, 277.

(23) Janoschek, R. F.; Fabian, W. M. F. *J. Mol. Struct.* **2003**, *661*–*662*, 635.

(24) Shamovsky, I. L.; Riopelle, R. J.; Ross, G. M. *J. Phys. Chem. A* **2001**, *105*, 1061.

(25) Nakahata, T. D.; Mulholland, J.; Sherrill, C. D.; Morokuma, K. Unpublished data, 2003.

(26) Asatryan, R. S.; Davtyan, A. H.; Khachatryan, L.; Dellinger, B. *J. Phys. Chem. A*, submitted for publication, 2004.

(27) Benson, S. W. *Thermochemical Kinetics*; John Wiley & Sons: New York, 1976.

(28) Wiater, I. J.; Born, G. P.; Louw, R. *Eur. J. Org. Chem.* **2000**, *6*, 921.

(29) Vol'eva, V. B.; Belostotskaya, J. S.; Ershov, V. V. *Izv. Akad. Nauk., Ser. Khim.* **1996**, *4*, 784.

(30) Sinnokrot, M. O.; Valeev, E. F.; Sherrill, C. D. *J. Am. Chem. Soc.* **2002**, *124*, 10887.

(31) Lin, C.-Y.; Lin, M. C. *Aust. J. Chem.* **1986**, *39*, 723.

(32) Emdee, J. L.; Brezinsky, K.; Glassman, I. *J. Phys. Chem.* **1992**, *96*, 2151.

(33) Ingham, T.; Walker, R. W.; Woolford, R. E. In *Proceedings of the Combustion Institute 25th Symposium (International) on Combustion*, Pittsburgh, PA, 1994; p 767.

(34) Brezinsky, K. M.; Pecullan, M.; Glassman, I. *J. Phys. Chem. A* **1998**, *102*, 8614.

(35) Kwok, E. C.; Atkinson, R.; Arey, J. *Environ. Sci. Technol.* **2000**, *29*, 1591.